Determination of Bimodal Molar Mass Distribution Functions of Polystyrene by Photon Correlation Spectroscopy: Numerical Simulations and Experimental Realization in Comparison with Gel Permeation Chromatography Data

Gyula Vancso,* Ivan Tomka, and Klara Vancso-Polacsek†

Institut für Polymere, Eidgenössische Technische Hochschule, CH-8092 Zürich, Switzerland. *Received March 25, 1987; Revised Manuscript Received July 31, 1987*

ABSTRACT: The resolution of bimodal molar mass distribution functions of polymers by photon correlation spectroscopy (PCS) combined with the constrained regularization method and the estimation of the noise level of PCS measurements is presented. Electric field autocorrelation functions for the scattered light on polymer solutions have been simulated. Molar mass distribution functions have been recalculated from the simulated autocorrelation functions. Simulation outputs show an increase of the polydispersity and a shift toward smaller molar masses with increasing statistical noise. The effective noise level of the present measurements was determined. Simulations show that with the effective noise level, two peaks of bimodal distributions can be resolved if the relative position of the constituents ($M2/M1$) is greater than 3. These simulations were compared with measured autocorrelation functions of bimodal molar mass distributions of certain mixtures of polystyrene standards ($M1 = 0.675 \times 10^6$, $M_w/M_n < 1.08$, and $M2 = 2.3 \times 10^6$, $M_w/M_n < 1.07$). The relative concentrations of the polystyrene standards $c(M1)/c(M2)$ were 1:1 and 1:0.4. The two constituents of the bimodal molar mass distribution functions were resolved for the two mixtures by PCS as predicted by the simulations. The peak- and weight-average molar masses as well as the relative amounts of the components of the bimodal distributions correspond to the anticipated values. GPC measurements were performed on the same samples. The distributions determined by PCS and GPC match each other reasonably well.

Introduction

The properties of high polymers are determined to a large extent by the molar mass and its distribution. However, there is no method for the analysis of the molar mass distributions of polymeric materials that is not limited to a particular molar mass range and by the complexity of the distribution functions.[1] In order to evaluate technologically important properties of linear, homopolymeric materials which are dependent on molar mass, it is necessary to analyze the molar mass distribution function (MMD) up to $1–3 \times 10^7$. The standard characterization method, gel permeation chromatography (GPC), cannot be applied for molar masses greater than $1–3 \times 10^6$ due to the lack of proper gels and GPC columns.[1] New methods of measurements are needed for the characterization of the higher molar masses. The application of photon correlation spectroscopy (PCS) to polymer solutions is not limited to the low molar mass range. Moreover, the increasing scattered intensity enhances the efficiency of this method with increasing molar mass.[1]

In the evaluation of autocorrelation functions several approximations are involved which are discussed in detail elsewhere.[2,3] The parameters of our experiments were selected so that the information contained in the measured autocorrelation functions is restricted to the translational movement of the macromolecular centers of mass. This condition is fulfilled if $qR_h < 0.4$, where $q = (4\pi n/\lambda) \sin(\theta/2)$ is the magnitude of the scattering vector, n is the refractive index of the solvent, λ is the wavelength of the incident light, θ is the scattering angle, and R_h is the (molar mass dependent) Stokes effective hydrodynamic radius.[4] The measured time autocorrelation function of the scattered light intensity, $g^{(2)}(t)$, has been estimated as

$$g^{(2)}(t) = B(1 + \gamma^2|g^{(1)}(t)|^2) \quad (1)$$

where B is the measured base line, γ is a parameter that characterizes the spatial coherence properties and the optical quality of the apparatus, and $g^{(1)}(t)$ is the electric field autocorrelation function.[2] Molar mass and center-of-mass translational diffusion coefficient of dissolved macromolecules are related:[2]

$$D = aM^{-b} \quad (2)$$

Taking into account relationship 2 and assuming that the refractive index increments for all macromolecular species are identical, the electric field autocorrelation function can be written[2] as

$$g^{(1)}(t) = \int G(t,M,q)f(M)\,dM + \epsilon(t) \quad (3)$$

where $f(M)$ is the normalized molar mass distribution function, $G(t,M,q)$ is a known function, and $\epsilon(t)$ is an unknown noise component of the measurements.[5] We used the scaling constants $a = 1.37 \times 10^{-4}$ and $b = 0.5$ (polystyrene in cyclohexane, 35 °C, see ref 6) for both the simulations and the evaluations of PCS measurements.

The inversion of (3) is an ill-posed mathematical problem;[7–10] i.e., $f(M)$ solutions can only be estimated. For the estimation of $f(M)$ the CONTIN program[8–11] was applied (see Appendix) which is based on constrained regularization. CONTIN delivers a set of possible solutions. In the Appendix we give a hint on how to select the most reliable one. According to ref 1 and 7, CONTIN is the most useful program available for determining moments as well as the complete molar mass distributions from PCS measurements.

Several studies have already been published concerning the determination of unimodal MMD of different polymers by PCS and we refer here only to some selected papers.[1,5,12–15] At the same time no data are available concerning noise level estimations and resolution of bimodal MMD functions of linear polymers by PCS compared with GPC data and with simulation predictions.

In the first part of this publication, the noise level of PCS measurements and the resolution power for a bimodal distribution are discussed with use of the results of computer simulations. The second part is devoted to the experimental realization of PCS and GPC measurements. In the third part, the efficiency of PCS is discussed especially

* To whom correspondence should be addressed.
† Present address: Projekt-Zentrum IDA, Eidgenössische Technische Hochschule, Zürich, Switzerland.

0024-9297/88/2221-0415$01.50/0

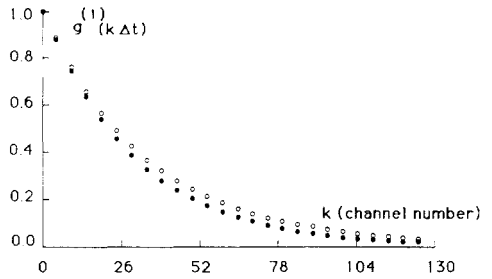

Figure 1. Simulated, noise-free, first-order autocorrelation functions of Poisson MMD functions: (○) bimodal distribution with $N1 = 20$ and $N2 = 80$; (●) unimodal distribution with $N^* = 50$.

for the determination of bimodal MMD functions using the simulated and measured data.

Simulation Studies

The advantage of using calculated autocorrelation functions is that one knows the correct molar mass distribution that should be found and one can add artificial noise with different amplitudes to the simulated autocorrelation functions. We report here on simulations using Poisson-type, bimodal molar mass precursor distribution functions. An anionic polymerization with ideal living character results in a Poisson distribution with a polydispersity index closed to 1.0.[16,17] This particular distribution was chosen because studies on anionic polystyrene polymerizates will be discussed in the Experimental Section. The simulated, noise-free autocorrelation functions were used as inputs for CONTIN runs. The MMD distribution functions resulting from CONTIN were compared with the precursor MMD functions.

The Simulation Procedure. Simulations were performed by using the following normalized precursor distribution function, $f(M)$:

$$f(N) = \frac{N_1{}^N e^{-N_1} + N_2{}^N e^{-N_2}}{2N^N e^{-N}(2\pi N)^{1/2}} \quad (4)$$

where N_1 and N_2 are the parameters (maxima) of the two constituent distributions, N is proportional to the degree of polymerization (see, i.e., ref 17), and $N!$ was approximated by the Stirling formula.

We calculated the noise-free, first-order autocorrelation function using $f(N)$ from eq 4 in 128 points (corresponding to the number of channels of our correlator) by evaluating the integral

$$g^{(1)}(t) \approx g^{(1)}(k\Delta t) = \frac{1}{M_w}\int_{M_{min}}^{M_{max}} M \exp(-q^2 k\Delta t a M^{-b}) f(M)\, dM \quad (5)$$

numerically using the Romberg procedure.[18]

Simulated, first-order, noise-free autocorrelation functions are compared in Figure 1. One of these functions was calculated for the bimodal, Poisson MMD with $N1 = 20$ and $N2 = 80$ and the other for a unimodal Poisson distribution with the parameter N^*, which is the arithmetic mean of $N1$ and $N2$. The difference between the two correlation functions has to be distinguished with sufficient precision by measurements to make the resolution of the two components possible.

A noisy, first-order autocorrelation function $G^{(1)}(t)$ was calculated by using the noise-free function (eq 5) according to the following expression:

$$G^{(1)}(k\Delta t) = [\gamma^2[g^{(1)}(k\Delta t) + \beta]^2 + \text{ERROR} \times [1 + \gamma^2[g^{(1)}(k\Delta t) + \beta]^2]^{1/2} \quad (6)$$

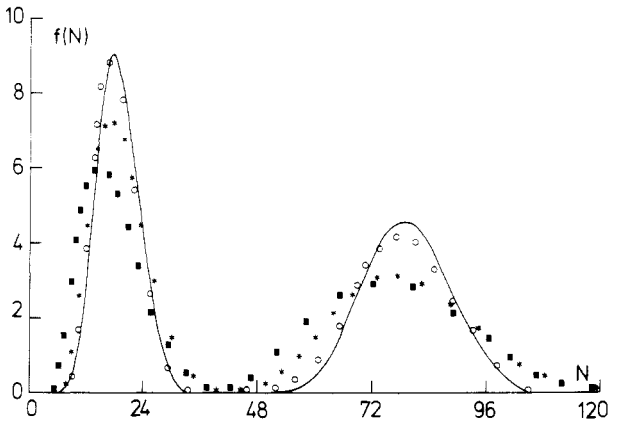

Figure 2. Simulations of bimodal, Poisson MMD functions with $N1 = 20$ and $N2 = 80$: solid line, precursor distribution. Outputs of CONTIN: (○) $R3 = 10^{-6}$; (*) $R3 = 10^{-4}$; (■) $R3 = 10^{-3}$.

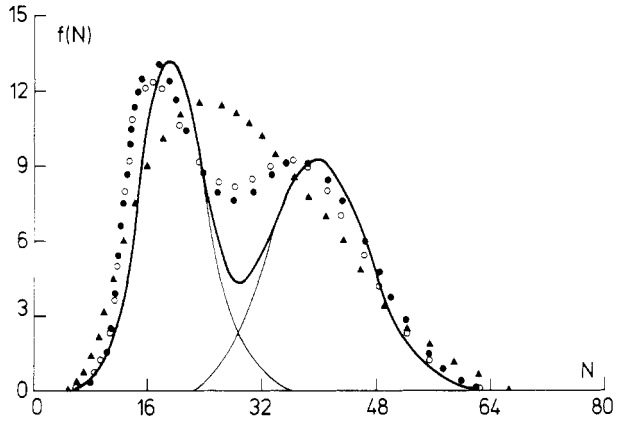

Figure 3. Simulations of bimodal, Poisson MMD functions with $N1 = 20$ and $N2 = 40$: solid line, distribution of the constituents; bold line, precursor bimodal distribution. Outputs of CONTIN: (●) $R3 = 10^{-7}$; (○) $R3 = 10^{-6}$; (▲) $R3 = 10^{-5}$.

where the error term is proportional to the intensity autocorrelation function, β describes the contribution of the dust, and ERROR is an adjustable parameter so that

$$\text{ERROR} = R3 \times RN(k) \quad (7)$$

where $R3$ is the noise parameter and $RN(k)$ is a random number distributed over the range (0;1) (see ref 5 and 8–11). With the proper selection of $R3$ any experimental noise can be approximated.

Results of the Simulations. Outputs from CONTIN for bimodal distributions with $N2/N1 = 4$ and $N2/N1 = 2$ and with different noise levels together with the precursor distributions (solid lines) are shown in Figures 2 and 3, respectively. (The simulated, noise-free autocorrelation function, which corresponds to the distribution with $N1 = 20$ and $N2 = 80$, was shown previously in Figure 1.) With noise-free autocorrelation functions as inputs for CONTIN, the outputs for both cases (see Figures 2 and 3) cannot be distinguished from the input (solid) curves for each grid point of the solution. From the solution set of CONTIN the so-called "chosen solutions" were selected for $N2/N1 = 2$ and $R3 < 10^{-4}$ and for $N2/N1 = 4$ and $R3 < 10^{-6}$. At higher noise levels, solutions were taken which meet better the a priori information (see Appendix).

Peak molar masses and polydispersity indices for the two constituents of the derived bimodal distributions are plotted respectively in Figures 4 and 5 as a function of the noise parameter. These plots show that significant distortion of the distribution (broadening and shift) first appears at $R3 \approx 10^{-4}$ and increases with increasing noise parameter.

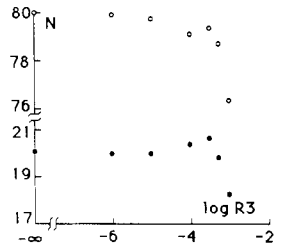

Figure 4. Peak molar masses of outputs of CONTIN of simulated, bimodal molar mass distributions as a function of the noise parameter: (●) $N1 = 20$; (○) $N2 = 80$.

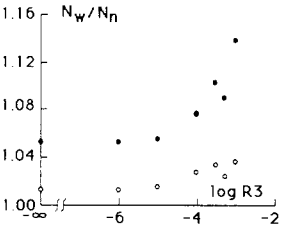

Figure 5. Polydispersity indices of outputs of CONTIN of simulated, bimodal, Poisson molar mass distributions as a function of the noise parameter: (●) $N1 = 20$; (○) $N2 = 80$.

As can be seen from Figures 2 and 3, there is already a slight deviation visible between the output of CONTIN and the input function, even at a very small noise level ($R3 \approx 10^{-6}$). The results show that both peaks of the bimodal distribution are shifted toward smaller molar masses and became broader with increasing noise parameter. This has also been observed for other distributions,[1] but the shift and distortion depend on polydispersity. The resolution limit of CONTIN in terms of the $R3$ noise parameter for $M2/M1 = 2$ can be established from Figure 3. The two peaks of the Poisson distributions with peak location ratio 2 cannot be resolved for noise levels higher than 10^{-5} although the two peaks separate well at lower noise values. At a peak location ratio of 4, CONTIN resolves the two constituents, even up to $R3 = 10^{-3}$ (see Figure 2). Significantly broader, most probable distributions located at M and $2M$ could not be separated even in the absence of added noise.[1]

We note that the present and other[1] simulations show that CONTIN delivers the moments of the input multimodal distribution function with an acceptable accuracy even for an unresolved output distribution.

Noise Level of Autocorrelation Functions. Each element of a solution set of CONTIN runs contains statistical parameters such as the objective function, variance, etc. CONTIN finally minimizes the objective function $V(\alpha)$ (as described in the Appendix), where $V(\alpha)$ is the sum of the squares of the errors plus a smoothing term. The noise statistics of the measurements have been characterized by checking $V(\alpha)$. This is not a rigorous characterization; it merely gives information about the deviation between the measured and fitted autocorrelation functions. The proper description would use the δ parameter (see Appendix, eq 10), which can be determined for the simulations but is unknown in experiments. However, the objective function can be used to estimate the noise level of the measurements in terms of $R3$ if the relationship between the $R3$ noise parameter and the objective function has previously been established.

Figure 6 shows some results of simulations concerning the dependence of $V(\alpha)$ on $R3$. These simulations were performed by using different precursor MMD functions (uni- and bimodal Dirac δ, Poisson, and most probable distributions, see ref 1). The polydispersity, modality, and

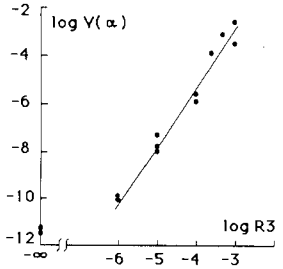

Figure 6. Relationship between the output objective function of CONTIN $V(\alpha)$ as a function of the input noise parameter $R3$ of simulation runs for different molar mass distributions.

shape of the simulated distributions (Poisson, most probable, Dirac δ) influence the objective function. However, a tentatively linear relationship on the log–log scale may be established for $R3 > 10^{-6}$. With this relationship and the objective function which corresponds to a given measurement, the noise level of experimental data can be estimated in terms of $R3$ (see Discussion). If $R3 < 10^{-6}$, the value of the objective function tends to the level of noise-free simulations and reaches a limiting value of about 10^{-11} (see Figure 6). The limiting value is a consequence of the numerical precision of our calculations ("computer noise"). It is about 8 orders of magnitude smaller than the objective function of the best experiments. Consequently, the "computer noise" does not influence our results. Our calculations were performed in double precision, which corresponds in our computer configuration to 29 decimal digits.

In general, it is possible to perform CONTIN simulations with different noise parameters for certain types of MMD functions to be measured. The objective functions of the simulation outputs may indicate whether the measurements using a concrete experimental setup are accurate enough for reliable estimations of the sought MMD function.

We emphasize again that the estimation of the effective $R3$ of an experiment involves a priori knowledge of the distribution to be studied. Care must be taken in making statements about error estimates since the errors in solutions to ill-posed problems are generally unbounded: only tendencies for the order of magnitude of $R3$ may be established by the estimation proposed in this publication.

Experimental Section

Two polystyrene samples prepared by anionic polymerization (Polymer Laboratories, LTD) were used in this study. Characteristics of the samples are as follows: $M1$, peak = 0.675×10^6 dalton, $M_w/M_n < 1.08$, $M2$, peak = 2.3×10^6 dalton, $M_w/M_n < 1.07$ (supplier's information). Measurements of the photon correlation function were performed by using a BI2030 multibit correlator from Brookhaven Inst. with a multiple sampling time option and with 128 channels. A Spectra-Physics Ar-ion laser Model 166 was used at the 514.5-nm line and with maximum power of 0.6 W. The detector was a Thorn-EMI type 9893A/100 photomultiplier. Typical measuring times were 10^3 s, with an average total photon count of about 5×10^7 at a scattering angle of 35°.

A cylindrical, fused-quartz sampling cell with an inside diameter of 8 mm was mounted at the center of a second, larger cylindrical quartz cell with a diameter of 90 mm. The gap between the two cells was filled with toluene to match the refractive index of the cells. Both vat and scattering cell were isolated from the environment by membrane filters. The temperature in the cuvette was adjustable up to 150 °C within ±0.1 °C accuracy. The samples were filtered through Teflon membrane filters directly into the scattering cell. Pore sizes were selected to be just large enough to allow through all PS species. For samples with $M1 = 0.675 \times 10^6$, 0.45-μm and, for 2.3×10^6, 1.2-μm pore size filters were used. PCS experiments were made with cyclohexane solutions

Table I
Nominal and Measured Relative Concentrations, Weight-Average Molar Masses, Polydispersity Indices, and the Corresponding Objective Functions of the CONTIN Runs for Components of Mixtures of Two Polystyrene Samples Measured by PCS

component 1 ($M1_{peak}$ = 0.675 × 10^6)[a]				component 2 ($M2_{peak}$ = 2.3 × 10^6)[a]				
nomin %	meas %	M_w	M_w/M_n	nomin %	meas %	M_w	M_w/M_n	$V(\alpha) \times 10^4$
100		7 × 10^5	1.07	0				2.5
0				100		2.5 × 10^6	1.12	6.0
50	50.5	6.8 × 10^5	1.19	50	49.5	2.4 × 10^6	1.07	2.3
71	72.9	6.6 × 10^5	1.20	29	27.1	2.2 × 10^6	1.06	1.4

[a] Supplier's specification.

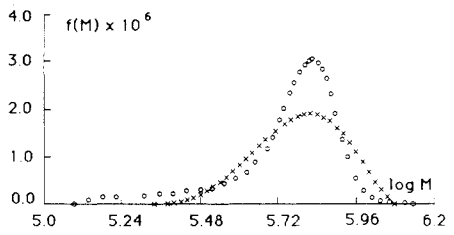

Figure 7. Molar mass distributions of a polystyrene standard with molar mass M_{peak} = 0.675 × 10^6 measured by GPC (O) and PCS (×).

of the polymers at the Θ temperature, 35.3 °C. The total polymer concentration was ≈1 mg cm^{-3}.

Care was taken in the proper setting of the spatial coherence since the number of coherence areas, A/A_{coh}, strongly influences the normalized value of the measured autocorrelation function.[19] A/A_{coh} was set with the optics of the photomultiplier so that we achieved typically for the first channel $g^{(1)}(1\Delta t) \approx 0.89$–$0.90$.

GPC spectra were recorded by using a home-filled, high-quality column with 40 000 theoretically equivalent plates per meter. The GPC column (16-mm inside diameter) was packed with the silica gel Merck SI 4000.[20]

The correlator was equipped with a Z80-based Super Quad microcomputer (Advanced Digital Corp.). Cumulant fits[21,22] were run by this computer to give a first estimate of the diffusion constant and polydispersity of the polymer solutions. The detected autocorrelation functions were then transferred into a CDC-CYBER 174/720 computer for analysis by CONTIN.

Experimental Results. Two mixtures of PS standards with relative concentration $c(M1)/c(M2)$ = 1:1 and $c(M1)/c(M2)$ = 1:0.4 as well as the single components ($M1$ and $M2$) were investigated. The supplier's specifications concerning the characteristics of the MMD were verified independently by Milton-Roy Co., Stone, GB, using a Chromatix low-angle laser light scattering (LALLS) detector and a GPC apparatus. Two series of LALLS measurements resulted for the peak molar masses of $M1_p$ = 0.681 × 10^6, 0.692 × 10^6 and of $M2_p$ = 2.2 × 10^6, 2.35 × 10^6. The agreement between these data and the supplier's information corresponds to the accuracy of GPC measurements (see ref 1).

The outputs of CONTIN for the individual constituents and the two mixtures are shown in Figures 7–10. GPC outputs measured on the same materials are plotted together with the PCS results. Those elements were chosen from the solution set of CONTIN which corresponded best to the supplier's specification concerning the peak-average molar masses. The differential MMD functions determined by GPC were calculated from the elution diagrams by using the transformation described by Pickett et al.[23] according to the equation

$$f(M) = \frac{1}{I} c(V_M) \frac{1}{[dH(V_M)/dV]_{V_M}} \frac{0.4343}{M} \qquad (8)$$

where $c(V_M)$ is the elution curve at the elution volume V_M corresponding to the molar mass M, I is the total area under $c(V)$, and $H(V_M) = \log M$ is the calibration relationship of the GPC column. All the MMD functions plotted in this paper are normalized, so that the total area under the MMD functions on the linear molar mass scale are equal to unity. Several characteristics of the outputs of GPC and PCS measurements are summarized in Table I.

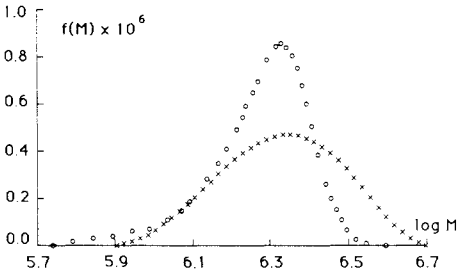

Figure 8. Molar mass distributions of a polystyrene standard with molar mass M_{peak} = 2.3 × 10^6 measured by GPC (O) and PCS (×).

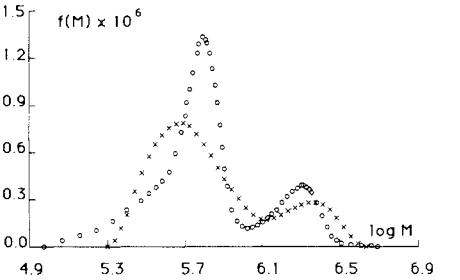

Figure 9. Bimodal molar mass distributions of mixtures of polystyrene standards with molar masses M_{peak} = 0.675 × 10^6 and M_{peak} = 2.3 × 10^6 and with 1:1 relative concentrations measured by GPC (O) and PCS (×).

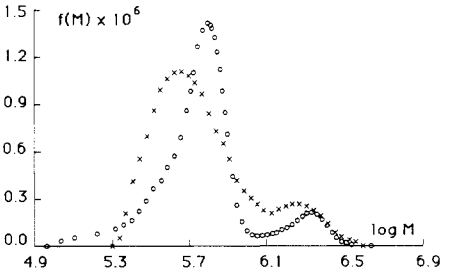

Figure 10. Bimodal molar mass distributions of mixtures of polystyrene standards with molar masses M_{peak} = 0.675 × 10^6 and M_{peak} = 2.3 × 10^6 and with 1:0.4 relative concentrations measured by GPC (O) and PCS (×).

The first two rows in Table I show results corresponding to the individual constituents of the bimodal distribution. The third and fourth row contain the results for the mixtures. The objective functions delivered by the CONTIN program which belong to the chosen outputs are also shown. The measured relative concentrations (measured percent) were determined by numerical integration of the MMD functions by CONTIN itself.

Discussion

A comparison of the GPC and PCS results shows that distributions determined by PCS are slightly broadened and shifted with respect to GPC spectra. The accuracy of the determination of the polydispersity by GPC is about 10%. The differences among the M_w/M_n values for the

components in Table I do not exceed this error significantly: the increase in the polydispersity index from the present PCS measurements due to the experimental noise is within this error.

The extent of the shift is a result of two competitive effects. The concentration dependence of the diffusion coefficient under Θ conditions is linear with a negative slope (see, e.g., ref 24 and references therein). This dependence, due to the finite concentration of the solutions, causes the molar masses to be shifted toward higher values when eq 2 is used to transfer from D to M. The experimental noise causes a shift in the opposite direction, i.e., toward smaller molar masses (see Part I, Results of Simulations). This trend can be seen on the shift of the peak with $M2$ molar mass which is larger in the 1:1 mixture (Figure 9) than in the 1:0.4 mixture (Figure 10). A reasonable explanation is that the concentration of the component with $M2$ in the 1:0.4 mixture is smaller and hence the shift due to the concentration dependence of D toward higher molar masses is also smaller. We always took the measured base line in order to eliminate the influence of dust. A shift in the MMD function due to dust is possible. On the other hand component 1 for measured bimodal distributions (i.e., mixture 1) is shifted to smaller molar masses while component 2 to higher values. This refers to a minor role of the dust in the shift.

Our experimental results indicate—by comparing the found $V(\alpha)$ values (Table I) with the data in Figure 6—that the noise level of our best measurements correspond to an $R3$ value close to 5×10^{-4}. This representative noise level of the experiments is also consistent with the resolution of two peaks experimentally (Figure 9, $M2/M1 = 3.5$) and by simulation (Figure 2, $N2/N1 = 4$) at $R3 < 10^{-3}$. We could not resolve the components of a bimodal MMD distribution with $M2/M1 = 2$. This supports the reliability of the noise level estimation of our experiments. An estimation of the overall experimental noise can be achieved only due to the fact that we had a priori knowledge of the MMD of the PS standards.

Conclusions

The limitations of photon correlation spectroscopy combined with the CONTIN program for the determination of molar mass distributions of polymers were discussed. The effective noise level of autocorrelation functions was estimated by performing simulations. It was found that an increase of the noise level broadens and shifts the distributions toward smaller molar masses.

Any experimental setup can be characterized with respect to effective noise levels by applying the proposed procedure. Simulations can be performed to decide whether a characterization of a given MMD function can be done under defined experimental conditions.

Our simulations and measurements show that bimodal, Poisson-like distributions with $M2/M1 > 3.5$ can be resolved if the corresponding effective noise level is smaller than 10^{-3}. Given that the peak-average molar masses are a priori information, polydispersity indices, weight-average molar masses, and relative amounts of the components of the bimodal distributions determined by PCS and GPC are in a reasonable agreement.

Acknowledgment. We acknowledge financial support from the Swiss National Scientific Foundation (Pr.-No. 2.046–0.86), from the Swiss Federal Institute for Technology, Zürich, and from Rheometrics Co., Piscataway, NY. We are indebted to Dr. R. F. T. Stepto for his critical reading of the manuscript and for helpful discussions. We thank B. Gut for performing the GPC measurements and Milton-Roy Co., Stone, GB, for the characterization of the samples.

Appendix

The constrained regularization method applied by Provencher[8-11] in the CONTIN program estimates the molar mass distribution function as a maximum of 100 grid points equally spaced along the log M axis. The program employs a constrained, weighted least-squares method (CWLSQ), taking into account statistical prior knowledge and the principle of parsimony. The objective function to be minimized is

$$V(\alpha) = \|g^{(1)}_{\text{calcd}}(t) - g^{(1)}_{\text{measd}}(t)\|^2 + \alpha^2 \int \frac{\mathrm{d}^2 f(M)^2}{\mathrm{d}M^2}\,\mathrm{d}M = V(0) + R \quad (9a)$$

where $\|...\|$ denotes the norm in the class of continuous, piecewise smooth functions. The constrained regularization as applied in CONTIN is a special case of the regularization method developed by Tihonov[25] where the objective function has the general form

$$V(\alpha) = \|g^{(1)}_{\text{calcd}}(t) - g^{(1)}_{\text{measd}}(t)\|^2 + \alpha_2 \int \sum_{j=1}^{p} \frac{\mathrm{d}^j f(M)^2}{\mathrm{d}M^j}\,\mathrm{d}M \quad (9b)$$

The value of the α regularization parameter determines the degree of smoothing of the solution and can only be set correctly if δ in the eq 10 is known:

$$\| \int G(t,M,q) f(M)_{\text{true}}\,\mathrm{d}M - g_{\text{measd}}{}^{(1)}(t) \| = \delta \quad (10)$$

There will generally be a large set of vectors $f(M_j)$ all of which satisfy eq 9 to within the experimental error, $\epsilon(t)$. Constraints can eliminate many unacceptable members of the solution set, but there are still many remaining with large variations from each other. CONTIN performs a series of solutions where α increases from a small value. The principle of parsimony says that one should take for the chosen solution the one with the largest α which is consistent with the data. However, on the basis of a priori information (number of peaks, knowledge of moments or other parameters, etc.) with regard to the searched solution, one may supervise the chosen solution and select another one which agrees better with the a priori information. Advice on how to select a "good" solution from a solution set from CONTIN has been provided by Provencher.[8-11]

Registry No. Polystyrene, 9003-53-6.

References and Notes

(1) Tomka, I.; Vancso, G. In *Applied Polymer Analysis and Characterization*; Mitchell, J., Jr., Ed.; Hanser: Munich 1987; and references therein.
(2) Berne, B. J.; Pecora, R. *Dynamical Light Scattering*; Wiley: New York, 1976. Greschner, G. S. *Maxwellgleichungen*; Hüthig and Wepf: Basel, 1981; Band 2.
(3) Tomka, I.; Vancso, G. *Polym. Prepr. (Am. Chem. Soc., Div. Polym. Chem.)* **1986**, *27*, 114.
(4) de Gennes, P.-G. *Scaling Concepts in Polymer Physics*; Cornell University Press: Ithaca, NY, 1979. Vancso, G. *Polym. Commun.* **1987**, *28*, 305.
(5) Provencher, S. W.; Hendrix, J.; MeMaeyer, L. *J. Chem. Phys.* **1978**, *69*, 4273.
(6) King, T. A.; Knox, A.; McAdam, J. D. G. *J. Polym. Sci., Polym. Symp.* **1974**, *44*, 195.
(7) Stock, R. S.; Ray, W. H. *J. Polym. Sci., Polym. Phys. Ed.* **1985**, *23*, 1393.
(8) Provencher, S. W. *Makromol. Chem.* **1979**, *180*, 201.
(9) Provencher, S. W. *Comput. Phys. Commun.* **1982**, *27*, 213.
(10) Provencher, S. W. *Comput. Phys. Commun.* **1982**, *27*, 229.
(11) Provencher, S. W. CONTIN *User's Manual*; EMBL: Heidelberg, 1982.

(12) Gulari, Erd.; Gulari, Es.; Tsunashima, Y.; Chu, B. *Polymer* **1979**, *20*, 347.
(13) Chu, B. *Polym. J.* **1985**, *17*, 225.
(14) Burchard, W. *Chimia* **1985**, *39*, 10.
(15) Vancso, G.; Tomka, I. *Polym. Prepr. (Am. Chem. Soc., Div. Polym. Chem.)* **1986**, *27*, 116.
(16) Flory, P. J. *Principles of Polymer Chemistry*; Cornell University Press: London, 1971.
(17) Peebles, L. H. *Molecular Weight Distributions in Polymers*; Wiley: New York, 1971.
(18) Davis, P. J.; Rabinowitz, P. *Methods of Numerical Integration*; Academic: New York, 1975; p 327.
(19) Jakeman, E.; Oliver, C. J.; Pike, E. R. *J. Phys. A: Gen. Phys.* **1970**, *3*, 145.
(20) Gut, B.; Tomka, I.; Vancso, G., manuscript in preparation.
(21) Koppel, D. E. *J. Chem. Phys.* **1972**, *57*, 4814.
(22) Pusey, P. N. In *Industrial Polymers: Characterization by Molecular Weight*; J. H., Green, R., Dietz, Eds.; Transcripta Books: London, 1973.
(23) Pickett, H. E.; Cantow, M. J. R.; Johnson, J. F. *J. Appl. Polym. Sci.* **1966**, *10*, 917.
(24) Vancso, G. *Polym. Bull.* **1986**, *16*, 551.
(25) Tihonov, A. N. *Sov. Math. Dokl. (Engl. Transl.)* **1963**, *4*, 1035, 1624.

Comparison of Correlation Lengths in Semidilute Polystyrene Solutions in Good Solvents by Quasi-Elastic Light Scattering and Small-Angle Neutron Scattering

Wyn Brown*

Institute of Physical Chemistry, University of Uppsala, Box 532, 751 21 Uppsala, Sweden

Kell Mortensen

Risø National Laboratory, DK-4000, Roskilde, Denmark. *Received March 31, 1987*

ABSTRACT: Quasi-elastic light scattering (QELS) and small-angle neutron scattering (SANS) experiments have been made on semidilute solutions of polystyrene (PS) in methylene chloride and tetrahydrofuran. The hydrodynamic screening length (ξ_H) from QELS and the excluded volume screening length (ξ) from SANS are found to be proportional at concentrations well above the dilute–semidilute crossover. The power law $C^{-0.68}$ applies to the static quantity whereas this asymptotic exponent value is only found for ξ_H with PS fractions of molecular weight $M \geq 10^6$. The dynamic length, ξ_H, is solvent independent while the static length is shown to be significantly shorter in methylene chloride ($\xi_H/\xi = 2.2$ in CH_2Cl_2 and 1.8 in THF), a result which is possibly related to differing extents of coil interpenetration in these solvents.

Introduction

Earlier investigations[1,2] of the dynamical behavior of semidilute solutions of high molecular weight polystyrenes in the good solvent, THF, indicated the presence of bimodal autocorrelation functions in QELS experiments. On theoretical grounds it had been anticipated that a unique correlation length, characterizing the homogeneous transient gel, would be reflected in single-exponential decay. On the other hand, preliminary measurements in another solvent, methylene chloride (CH_2Cl_2), of equivalent solvating power gave the expected narrow line width when using the same samples and with the same measurement parameters. A possible explanation is that there are differences in the extent of coil interpenetration in these solvents. This aspect has recently received attention in neutron scattering experiments[3] and in a novel study using a fluorescence method.[4] These data lend support to the earlier conclusions of Dautzenberg[5] that an overlapping of the internal cores of polymer coils does not occur to the same extent. We note also the similar results given by computer simulations.[6]

A more detailed comparison of the screening lengths of PS in these and other solvents seemed warranted. The possible existence of multiple lengths in semidilute solutions is far from trivial since it calls into question fundamental assumptions on which scaling theory is formulated and which lead to predictions of the universality of solution behavior.

From the notation of Edwards,[7,8] ξ and ξ_H are respectively the screening lengths for the excluded-volume and hydrodynamic interactions. The excluded-volume effect is a static quantity which in semidilute solutions is accessible to measurement by using small-angle neutron scattering (SANS) or small-angle X-ray scattering (SAXS). The dynamic quantity may be obtained by using QELS or with samples of lower molecular weight by using the neutron spin–echo technique. Past studies have emphasized the testing of the power law predictions for the concentration dependence of the correlation length (or cooperative diffusion coefficient). According to scaling theory,[9] ξ is related to the concentration, C, by

$$\xi \sim C^{-\nu/(3\nu-1)} \quad (1)$$

where ν is the excluded-volume exponent in the relationship $R_g \sim M^\nu$ (where R_g is the gyration radius and M molecular weight). For good solvents, $\nu = 0.6$ in the limit of infinite M, which leads to a concentration exponent of -0.75 in eq 1. However, numerous experimental investigations (see, for example, ref 1 and 10–15) have established a value of about -0.67 for both ξ and ξ_H.

Differences in the absolute values of ξ and ξ_H and their ratio have received less attention. These quantities were implied by de Gennes[9] to be identical whereas Muthukumar and Edwards[8] stress the essential physical difference between them.

This paper is directed partly to an examination of the behavior of PS in CH_2Cl_2 in greater detail than hitherto and partly to a comparison of the screening lengths in this solvent and THF. Both QELS and SANS measurements have been made over the semidilute regime on essentially monodisperse PS fractions.

Experimental Section

Polystyrene samples (PSH) and deuteriated polystyrene (PSD) with the same molecular weight (1.01×10^5) were obtained

0024-9297/88/2221-0420$01.50/0